The TLK-ASF1 histone chaperone pathway plays a critical role in IL-1β–mediated AML progression

Hsin-Yun Lin,[1-5] Mona Mohammadhosseini,[1-5] John McClatchy,[1-5] Marina Villamor-Payà,[6,7] Sophia Jeng,[8] Daniel Bottomly,[8] Chia-Feng Tsai,[9] Camilo Posso,[9] Jeremy Jacobson,[9] Andrew Adey,[1,4] Sara Gosline,[9,10] Tao Liu,[9] Shannon McWeeney,[1,8] Travis H. Stracker,[6,7] and Anupriya Agarwal[1-5]

[1]Knight Cancer Institute, [2]Division of Hematology and Oncology, [3]Department of Oncogenic Science, [4]Department of Molecular and Medical Genetics, and [5]Department of Cell, Developmental and Cancer Biology, Oregon Health & Science University, Portland, OR; [6]Institute for Research in Biomedicine, Barcelona Institute of Science and Technology, Barcelona, Spain; [7]Radiation Oncology Branch, National Cancer Institute, National Institutes of Health, Bethesda, MD; [8]Division of Bioinformatics and Computational Biology, Oregon Health & Science University, Portland, OR; [9]Biological Science Division, Pacific Northwest National Laboratory, Richland, WA; and [10]Department of Biomedical Engineering, Oregon Health & Science University, Portland, OR

KEY POINTS

- **TLK and ASF1 levels are elevated in patients with AML across genetic subtypes and upregulated by IL-1β–mediated inflammatory stress.**
- **Targeting TLK2 or ASF1B suppresses IL-1β–driven AML progression through regulation of cell cycle and DNA damage responses in AML.**

Identifying and targeting microenvironment-driven pathways that are active across acute myeloid leukemia (AML) genetic subtypes should allow the development of more broadly effective therapies. The proinflammatory cytokine interleukin-1β (IL-1β) is abundant in the AML microenvironment and promotes leukemic growth. Through RNA-sequencing analysis, we identify that IL-1β–upregulated *ASF1B* (antisilencing function-1B), a histone chaperone, in AML progenitors compared with healthy progenitors. ASF1B, along with its paralogous protein ASF1A, recruits H3-H4 histones onto the replication fork during S-phase, a process regulated by Tousled-like kinase 1 and 2 (TLKs). Although ASF1s and TLKs are known to be overexpressed in multiple solid tumors and associated with poor prognosis, their functional roles in hematopoiesis and inflammation-driven leukemia remain unexplored. In this study, we identify that ASF1s and TLKs are overexpressed in multiple genetic subtypes of AML. We demonstrate that depletion of *ASF1s* significantly reduces leukemic cell growth in both in vitro and in vivo models using human cells. Using a murine model, we show that overexpression of ASF1B accelerates leukemia progression. Moreover, *Asf1b* or *Tlk2* deletion delayed leukemia progression, whereas these proteins are dispensable for normal hematopoiesis. Through proteomics and phosphoproteomics analyses, we uncover that the TLK-ASF1 pathway promotes leukemogenesis by affecting the cell cycle and DNA damage pathways. Collectively, our findings identify the TLK1-ASF1 pathway as a novel mediator of inflammatory signaling and a promising therapeutic target for AML treatment across diverse genetic subtypes. Selective inhibition of this pathway offers potential opportunities to intervene effectively, address intratumoral heterogeneity, and ultimately improve clinical outcomes in AML.

Introduction

Acute myeloid leukemia (AML) is one of the deadliest hematologic malignancies. Genetic heterogeneity within and between patients is an ongoing challenge for treating AML. For decades, conventional chemotherapies have served as the standard of care for patients with AML.[1] Despite the development of targeted therapies against common mutations, such as FMS-related tyrosine kinase 3 (FLT3), the emergence of drug-resistant mutations and therapeutic resistance remains a major obstacle.[2] Furthermore, the bone marrow microenvironment plays a critical role in AML progression, providing a supportive niche for leukemic cells and contributing to therapeutic resistance.[3] Therefore, targeting common pathways regulated by the bone marrow microenvironment may provide a promising therapeutic strategy to overcome intratumoral heterogeneity and therapeutic resistance, and improve the outcomes in patients with AML.

Recent studies have highlighted the association between infectious or autoimmune diseases and an increased risk for myelodysplastic syndrome and AML, underscoring the involvement of the microenvironment in disease development.[4-6] Importantly, we, and others, found that the bone marrow microenvironment in AML is inflammation rich and exerts inflammatory stress on healthy and leukemic

hematopoietic stem and progenitor cells. Specifically, we have identified that the proinflammatory cytokine interleukin-1β (IL-1β) is elevated in patients with AML, which promotes leukemic cell growth while suppressing the growth of healthy progenitors.[7] Furthermore, several downstream effectors of IL-1β signaling, including IL-1RAP, IRAK1, and TRAF6, have been implicated in AML and myelodysplastic syndrome, and targeting these molecules has shown potential in impairing leukemic cell survival.[8-10]

ASF1A and ASF1B are paralogous histone chaperones responsible for delivering histone H3-H4 to the replication fork during DNA replication, transcription, and DNA damage repair.[11,12] These histone chaperones are substrates for Tousled-like kinases 1 and 2 (TLK1 and TLK2), which are paralogous kinases essential for DNA replication and repair.[13,14] Phosphorylation of ASF1 by TLKs promotes binding and delivery of the histone H3-H4 dimer.[14-17] Notably, elevated expression of both ASF1 and TLK has been observed in a variety of cancers, including breast cancer, and is associated with a poor prognosis.[18-20] In this study, we sought to investigate the involvement of the TLK-ASF1 pathway in AML progression. We demonstrated that both TLKs and ASF1s are highly expressed in AML cells compared with healthy cells, and this upregulation was further enhanced under IL-1β–mediated inflammatory stress. Subsequently, we examined the impact of TLK and ASF1 depletion on AML cell growth using in vitro and in vivo models, aiming to evaluate their potential as therapeutic targets in AML. By unraveling the intricate interplay between inflammation and the TLK-ASF1 pathway in AML, our findings contribute to a deeper understanding of AML pathobiology and establish a solid foundation for the development of targeted therapeutic interventions against this devastating disease.

Methods

Primary samples

Peripheral blood or bone marrow of primary AML samples were obtained from Oregon Health and Science University (OHSU) Beat AML biorepositories and patients consented following the institutional review board guidelines. All samples represented unique patients with AML and the clinical, genetic, and demographic information of patient samples are summarized in supplemental Table 1, available on the *Blood* website. The details for primary sample purification and culturing are described in the supplemental Methods.

Gene expression analyses

Messenger RNA (mRNA) of purified $CD34^+$ cells from patients with AML and healthy donors (purchased commercially from Lonza Inc) was extracted using miRNeasy micro kit following the manufacturer's protocol. RNA sequencing (RNA-seq) analyses and TaqMan low-density array (TLDA) were used as described in the supplemental Methods.

Cell line generation, cell-based assays, and xenograft study

MOLM-14 cells expressing short hairpin RNA (shRNA) targeting *TLK1*, *TLK2*, *ASF1A*, and *ASF1B*, and 2 nonspecific controls (NT16 and NT17) were generated using lentivirus. Upon ASF1 and TLK knockdown, colorimetric MTS [3-(4,5-dimethylthiazol-2-yl)-5-(3-carboxymethoxyphenyl)-2-(4-sulfophenyl)-2H-tetrazolium] cell viability, cell growth, cell cycle, and colony formation assays were performed. In vivo, the effect of ASF1 knockdown was assessed using nonobese diabetic/severe combined immunodeficiency $IL2R\gamma^{-/-}$ (NSG) mice, and is described in the supplemental Methods.

Mice

All animal studies were approved by OHSU institutional animal care and use committee. Animals were housed at the OHSU semiconventional facility. *Asf1b*$^{em1(IMPC)J}$ (MMRRC stock 42325), *Vav-iCre* (JAX stock 008619), and C57BL/6 mice were purchased from The Jackson Laboratory. *Tlk2*$^{fl/fl}$ mice[21] were crossed with *Vav-iCre* mice to generate *Vav-Cre*$^+$*Tlk2*$^{fl/+}$ and *Vav-Cre*$^+$*Tlk2*$^{fl/fl}$ hematopoietic-specific conditional knockout mice. For genotyping, tail tips were collected at weaning and analyzed by quantitative real-time polymerase reaction (Transnetyx).

Bone marrow transplantation

Bone marrow cells were isolated from bones of 6- to 8-week-old *Asf1b*$^{+/+}$, *Asf1b*$^{+/-}$, *Asf1b*$^{-/-}$, *Vav-Cre*$^-$*Tlk2*$^{fl/fl}$, *Vav-Cre*$^+$*Tlk2*$^{fl/+}$, and *Vav-Cre*$^+$*Tlk2*$^{fl/fl}$ donor mice. Bone marrow transplantations were performed as described previously[22-24] and in the supplemental Methods.

Proteomics and phosphoproteomics

Global proteomics and phosphoproteomics analysis of AML cell line MOLM-14 were performed upon knockdown of ASF1s or TLKs as described in the supplemental Methods.

Statistical analysis

Variables were compared by pairwise Student 2-tailed *t* test assuming homoscedastic variances. Fisher exact test was used for categorical variables, and Mann-Whitney *U* test was used for continuous variables. The level of significance was set at *P* value $\leq .05$.

Results

Gene expression profiling identifies ASF1B upregulation in AML progenitors upon IL-1β stimulation

We previously found that aberrant IL-1β signaling promotes the growth of AML progenitors and leukemogenesis.[7] To reveal the cell-intrinsic mechanisms downstream of IL-1β signaling in AML, we performed RNA-seq analysis of AML and healthy bone marrow $CD34^+$ progenitors treated with and without IL-1β from 3 independent patient samples. We identified 66 differentially expressed genes in AML progenitors and healthy progenitors upon IL-1β exposure compared with vehicle-treated controls (false discovery rate of <0.05, supplemental Tables 2 and 3). Upon IL-1β stimulation, 46 genes were only upregulated in AML progenitors (Figure 1A), 7 genes were only upregulated in healthy progenitors, and 12 genes were upregulated in both. In addition, *VCAN* was the only gene that was significantly downregulated in healthy progenitors.

Gene ontology analysis using STRING-DB[25] revealed that 46 of 65 upregulated genes in AML progenitors upon IL-1β stimulation belong to biological processes including chromosome organization (*ASF1B*, *MAD2L1*, and *HIRIP3*), cytokine-mediated signaling (*TNFRSF9*, *BIRC3*, and *MMP9*), as well as cell cycle (*CDCA3*, *CEP55*, and *RRM2*; Figure 1B; supplemental Tables 2

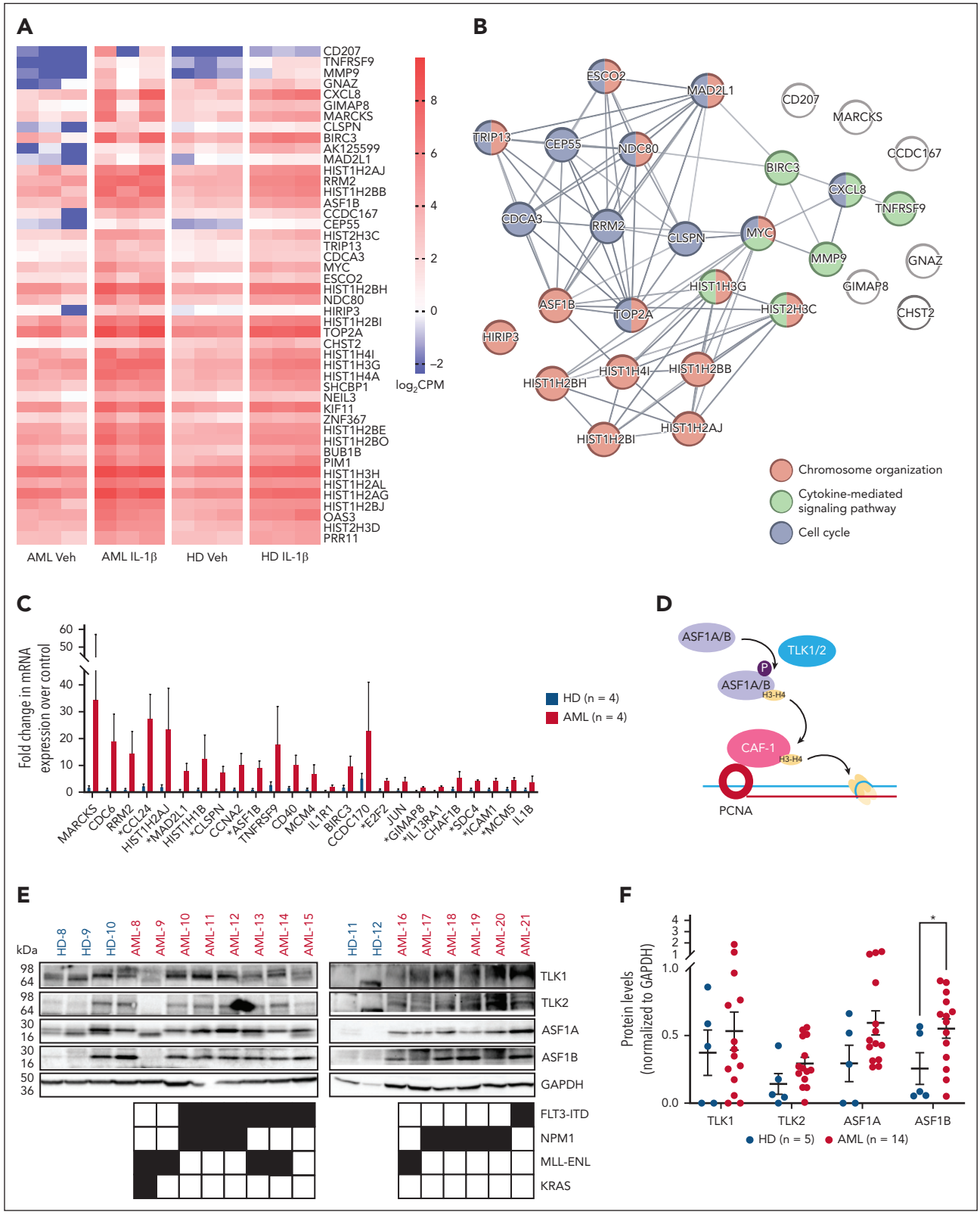

Figure 1. ASF1B is upregulated in AML progenitors upon IL-1β stimulation. (A) RNA-seq analysis was performed using purified CD34$^+$ cells derived from the bone marrow of patients with AML (n = 3) and healthy donors (n = 3). Cells were cultured with 10 ng/mL IL-1β or vehicle control for 2 days. The heat map indicates $\log_2$ counts per million (CPM) of differentially expressed genes in vehicle- or IL-1β–treated healthy and AML CD34$^+$ bone marrow cells. (B) STRING-DB network analysis of genes upregulated in IL-1β–treated AML cells vs IL-1β–treated healthy cells. (C) TLDA analysis was performed on AML (n = 4) and healthy CD34$^+$ (n = 4) bone marrow cells treated with or without 10 ng/mL IL-1β for 2 days. The expression of listed genes is shown as a fold difference upon IL-1β stimulation compared with respective vehicle controls in AML and healthy CD34$^+$ bone marrow cells. (D) Schematic representation of the TLK-ASF1 pathway. (E) Immunoblot of TLKs and ASF1s protein expression in CD34$^+$ bone marrow cells from healthy donors (n = 5) and patient-derived AML samples (n = 14) with indicated mutations. (F) Densitometry analysis of the immunoblot is shown and expressed as means ± standard error of the mean (SEM). Student *t* test was used for statistical analysis. *P < .05.

and 3). We confirmed our findings from RNA-seq analysis using the TLDA to assess the expression of top differentially expressed genes and genes associated with the IL-1β signaling in additional samples from patients with AML harboring diverse genetic mutations such as FLT3-ITD and NPM1 (supplemental Table 4; Figure 1C). Consistent with our RNA-seq data, TLDA revealed that *ASF1B* has larger fold changes in AML vs healthy progenitors (Figure 1C). Higher ASF1B expression is associated with poor prognosis in solid tumors, such as breast and cervical cancer.[18,26,27] However, its role in hematopoiesis and leukemia is unclear. Therefore, we focused on understanding the role of ASF1B in AML progression at a steady state and under inflammatory stress.

Expression of ASF1 and TLK is upregulated in AML across genetic subtypes

ASF1B and its paralogue ASF1A are regulated by TLK1 and TLK2 (Figure 1D),[14] which are amplified in several types of solid tumors.[19,20] Therefore, we first quantified the TLK and ASF1 levels in healthy $CD34^+$ progenitor cells, as compared with AML cells derived from patients with common genetic mutations and translocations including FLT3-ITD, NPM1, and MLL-ENL (Figure 1E). We found that ASF1B levels were significantly higher (2.2-fold) in AML than in healthy progenitors. Additionally, the expression of TLK2, TLK1, and ASF1A exhibited an increasing trend (2.1-, 1.4-, and 2-fold, respectively) due to variations in different patient samples (Figure 1E-F). TLK1, TLK2, ASF1A, and ASF1B were also highly expressed across various AML cell lines (supplemental Figure 1A). Accordingly, the DepMap CRISPR database analysis[28] shows that most AML cell lines are highly dependent on ASF1B, ASF1A, and TLK2, whereas less dependent on TLK1 (supplemental Figure 1B). Importantly, patients with AML with higher *ASF1B* expression showed poor survival in the BeatAML database (supplemental Figure 1C). Furthermore, similar to our previous study[7] in which IL1R1 expression is not correlative of genetic subtypes, most AML genetic subtypes did not correlate with high *ASF1B* expression in AML[29] except the presence of KRAS mutations in patients was correlated with higher *ASF1B* expression (supplemental Figure 1D). These results suggested a broader role of TLKs and ASF1s across various genetic subtypes. Of note, *TLK1*, *TLK2*, and *ASF1A* transcript levels were not significantly different across patients with AML (data not shown) but increased at protein level (Figure 1E). Together, these results indicated that patients with AML have aberrant protein expression of TLKs and ASF1s.

IL-1β–mediated regulation of TLK-ASF1 pathway in AML

We observed that IL-1β stimulation upregulated *ASF1B* transcript levels in AML progenitors (Figure 1A,C; supplemental Figure 2A). We sought to assess whether IL-1β directly upregulates *TLK1* and *TLK2* mRNA expression (supplemental Figure 2A). Although there was no increase in the expression of *TLK1*, an increasing trend for *TLK2* transcripts upon IL-1β stimulation was observed. TLK1 and TLK2 levels are upregulated in AML at the protein level upon IL-1β stimulation. Additionally, consistent with increased TLK1 and TLK2 levels, ASF1B and pASF1A levels are increased (Figure 1E; supplemental Figure 2B). Our previous study showed that IL-1β promoted AML cell growth through the activation of the downstream p38MAPK.[7] Next, we determined whether p38MAPK regulated the TLK-ASF1 pathway in response to IL-1β. Blockade of p38MAPK (doramapimod or ralimetinib) abolished IL-1β–induced *ASF1B* expression at mRNA levels, as compared with vehicle-treated AML samples (supplemental Figure 2A). Blockade of p38MAPK did not alter TLK1 or TLK2 expression with and without stimulation of IL-1β (supplemental Figure 2A-B). These results suggest that ASF1B is downstream of IL-1β and p38MAPK. Enrichr analysis[30] for the ChIP enrichment analysis data set, using genes that are upregulated by IL-1β in AML progenitors (Figure 1B), suggested that *ASF1B* may be regulated by several transcription factors including E2F4, FOXM1, MYBL2, and E2F1, the known regulators of *ASF1B*[31] (supplemental Figure 2C; supplemental Table 5). Published chromatin immunoprecipitation sequencing data analysis[32] showed that E2F4, FOXM1, MYBL2, and E2F1 occupy the *ASF1B* promoter (supplemental Figure 2D), suggesting a direct regulation. Analysis of The Cancer Genome Atlas data indicated that the expression of both *E2F1* and *MYBL2* strongly correlated with high *ASF1B* expression in patients (supplemental Figure 2E).[33] Similar to ASF1 and TLK genes, many AML cell lines showed a high dependency on *MYBL2* and *E2F1* expression (supplemental Figure 2F).[28] Blockade of p38MAPK phosphorylation abolished IL-1β–mediated expression of MYBL2 and E2F1, similar to *ASF1B* (supplemental Figure 2G). Together, these data suggest that IL-1β may upregulate ASF1B through multiple transcription factors, which is downstream of p38MAPK.

The absence of ASF1 suppresses the growth and leukemia burden of AML

To determine the role of ASF1 in AML, we depleted *ASF1A*, *ASF1B*, or both, using doxycycline-inducible, shRNAs in MOLM-14 cells, which harbor FLT3-ITD mutation, one of the most common mutations in AML (Figure 2A-B). Depletion of *ASF1A* or *ASF1B* impaired MOLM-14 viability and cell growth (Figure 2C-D). The effect of the combined knockdown of both ASF1A and ASF1B was similar to the knockdown of ASF1B alone, suggesting that ASF1B may compensate for the loss of ASF1A in ASF1A-depleted cells (Figure 2C-D). In addition to MOLM-14 cells, we also depleted *ASF1A*, *ASF1B*, or both proteins in MONOMAC-1 cells. We observed reduced viability (supplemental Figure 3A-B) upon the knockdown. However, no changes were observed using nontargeting hairpins (supplemental Figure 3B-D). Cell cycle analysis demonstrated that a proportion of cells accumulated at G0/G1 phase, accompanied by decreased S and G2/M phase populations upon knockdown of ASF1A, ASF1B, or both, suggesting impaired progression from G0/G1 to S phase or cell cycle exit (Figure 2E). Consistent with proliferative defects and cell cycle arrest, the depletion of *ASF1A*, *ASF1B*, or both, resulted in a 2.5- to 5-fold reduction in colony formation assay compared with controls (Figure 2F). To examine the effect of *ASF1* depletion in vivo, MOLM-14 cells expressing shASF1A (red fluorescent protein–positive [RFP^+]), shASF1B (green fluorescent protein–positive [GFP^+]), and shASF1A/B (GFP^+RFP^+) were xenografted into NSG mice and assessed for leukemic burden (Figure 2G). Using RFP/GFP and MOLM-14 cell surface markers $CD13^+CD33^+$ and $CD15^+$, we found that ASF1 knockdown reduced the leukemic burden by 80% to 90% in the bone marrow compared with controls (Figure 2H-I). Spleen weight in the doxycycline-treated group was reduced by 80% compared

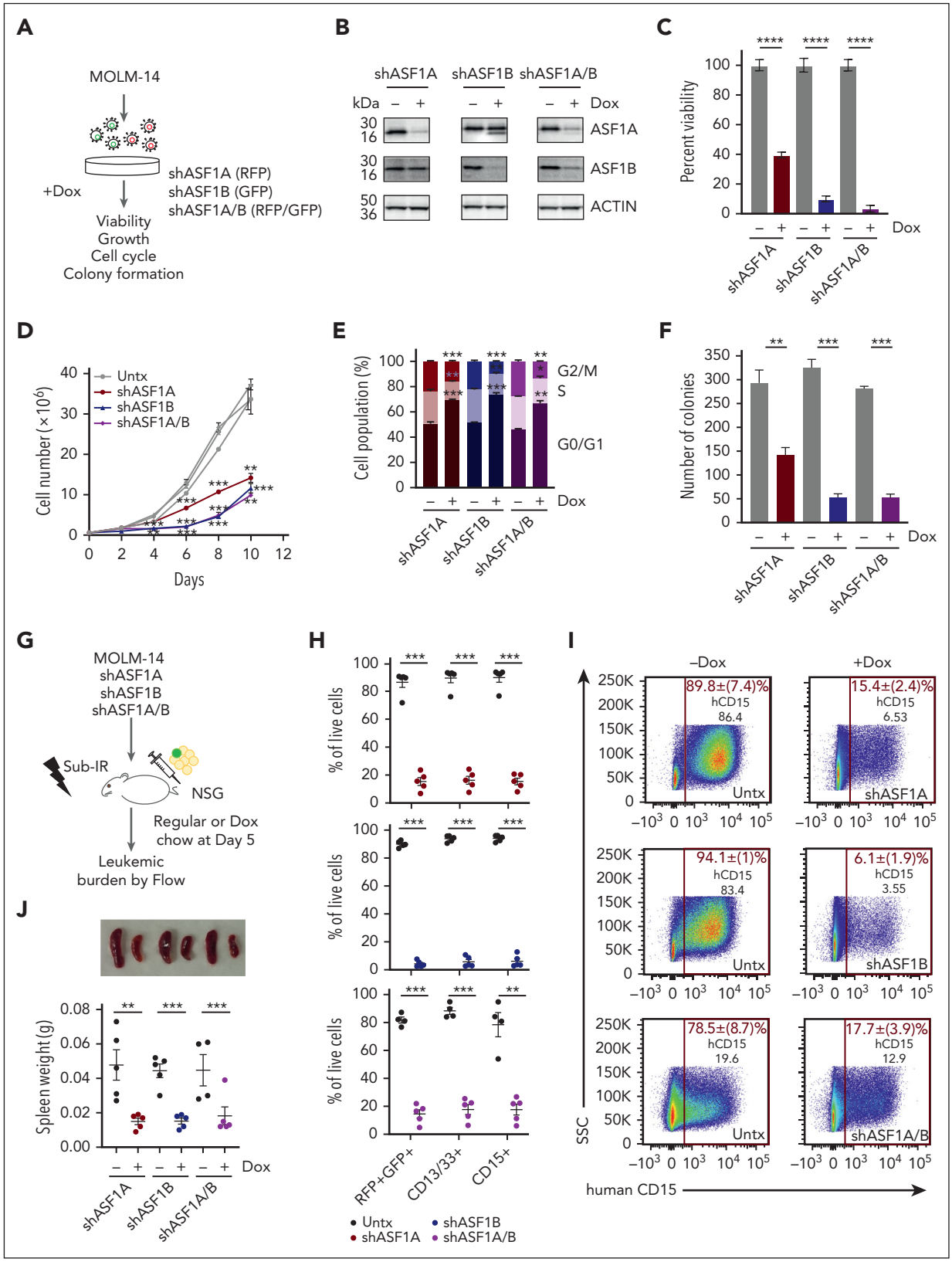

Figure 2. Reduced ASF1 levels suppressed in vitro and in vivo AML growth and leukemia burden using human cells. (A) A schematic representation of a doxycycline-inducible shRNA model targeting *ASF1A*, *ASF1B*, or both *ASF1A* and *ASF1B* in MOLM-14 cells. (B) MOLM-14 cells were treated with 1 μg/mL doxycycline to induce knockdown for 6 days. The effect of the knockdown was measured by immunoblotting analysis. shRNA expressing cells were kept in doxycycline-containing media throughout the culture. (C) Cell viability of MOLM-14 cells expressing shASF1A, shASF1B, or both was measured by colorimetric (MTS) assays after 6 days of doxycycline-induced knockdown. (D) Cell growth over time of MOLM-14 cells expressing shASF1A, shASF1B, or both was indicated by cell counts. (E) Cell cycle analysis of MOLM-14 cells expressing shASF1A, shASF1B, or both using propidium iodide and flow cytometry after 3 days of doxycycline-induced knockdown. (F) Colony formation assay was assessed

with controls (Figure 2J). MOLM-14 cells expressing nontargeting shRNA (shNT16 or shNT17) were xenografted into NSG mice, and we observed no significant differences in leukemic burden in doxycycline-treated and untreated groups (supplemental Figure 3E-F). Similarly, we found a reduction in the viability of primary AML cells upon ASF1A and ASF1B knockdown (supplemental Figure 3G). Collectively, these results indicate that ASF1A or ASF1B can potentiate AML cell growth and that targeting either was sufficient to impair AML growth.

ASF1B is a mediator of IL-1β–driven AML progression

Depmap analysis showed that AML cell lines with broader genetic subtypes were more dependent on *ASF1B* than *ASF1A*. Next, to test whether IL-1β promotes AML progression by regulating the expression of *ASF1B*, we used a murine bone marrow transplantation model of AML driven by an oncogenic fusion protein, MLL-ENL.[34] We transduced wild-type bone marrow cells with retrovirus expressing MLL-ENL and GFP, along with retrovirus expression of ASF1B and mCherry, or mCherry alone as an empty-vector control. Sorted double-positive cells were subsequently transplanted into lethally irradiated recipient mice that were treated with IL-1β or vehicle daily via intraperitoneal injection after transplantation (Figure 3A). We found that mice treated with IL-1β succumbed to the disease rapidly (median survival, 64 days; range 31-80 days), compared with the vehicle-treated mice (median survival, 85 days; range, 63-112 days; $P = .028$). Notably, ectopic ASF1B expression shortened survival (median survival, 62 days; range, 36-84 days; $P = .024$), mimicking IL-1β–mediated AML progression. However, ASF1B overexpression with IL-1β treatment did not further accelerate disease progression compared with ASF1B alone, possibly because of the saturation of ASF1B levels (Figure 3B). At 5 to 7 weeks after transplant, we observed a higher percentage of leukemic cells in the peripheral blood of ASF1B-overexpressing recipients (supplemental Figure 4A). At the terminal stage, spleen weights were comparable between each group (supplemental Figure 4B) and all the mice showed myeloid expansion of leukemic cells in the bone marrow (supplemental Figure 4C). Taken together, these results suggest that IL-1β treatment or ASF1B overexpression promoted myeloid expansion and leukemia progression. To further evaluate whether ASF1B plays a role in IL-1β–mediated AML progression, we performed complementary studies using *Asf1b*$^{-/-}$ mice. We first assessed the impact of *Asf1b* deficiency in normal hematopoiesis and observed no significant difference in differential blood counts of *Asf1b*$^{+/+}$, *Asf1b*$^{+/-}$, and *Asf1b*$^{-/-}$ mice (supplemental Figure 4D). Accordingly, flow cytometry analysis of bone marrow cells showed no significant difference in hematopoietic lineages or stem and progenitor cell populations (Figure 3C), suggesting that there are no major hematopoietic defects in *Asf1b*-deficient cells. Additionally, we performed 1:1 competitive growth assay in vitro, and we observed that *Asf1b*$^{-/-}$ cells have a slight growth advantage up to day 5 in culture but reduced their growth on day 11. Thus, we did not observe consistent growth differences between *Asf1b*$^{+/+}$ and *Asf1b*$^{-/-}$ cells over time (supplemental Figure 4E). These results are consistent with the immunophenotyping data from these mice (Figure 3C).

To determine whether *Asf1b* deletion suppresses leukemogenesis and IL-1β–mediated progression in vivo, we transplanted *Asf1b*$^{+/+}$, *Asf1b*$^{+/-}$, and *Asf1b*$^{-/-}$ cells expressing MLL-ENL and GFP into lethally irradiated recipients (Figure 3D). Heterozygous and homozygous *Asf1b* deficiency (median survival, 68 and 67 days, respectively; range, 58-84 and 60-84 days, respectively) extended survival of leukemic mice compared with wild-type mice (median survival, 62 days; range, 47-68 days). Notably, *Asf1b* deficiency attenuated IL-1β–mediated leukemia progression (Figure 3E) (median survival, 63 vs 47 days, respectively; range, 53-67 and 40-61 days, respectively). Additionally, IL-1β–treated *Asf1b*$^{+/+}$ mice have shorter survival than vehicle-treated *Asf1b*$^{+/+}$ mice (median survival, 47 and 62 days, respectively; $P = .006$) (supplemental Figure 4F). IL-1β–treated *Asf1b*$^{-/-}$ mice have slightly shorter survival than vehicle-treated *Asf1b*$^{-/-}$ mice (median survival, 63 and 67, respectively; $P = .046$) (supplemental Figure 4F). IL-1β shortened the survival of *Asf1b*$^{+/+}$ mice to a greater extent compared with survival of *Asf1b*$^{-/-}$ mice (Figure 3E). It is possible that other proteins regulated by IL-1β also play roles in AML progression in the absence of ASF1B. At 8 weeks after transplant, we observed a lower percentage of leukemic cells in the peripheral blood of *Asf1b*$^{+/+}$ and *Asf1b*$^{-/-}$ recipients (supplemental Figure 4G). A slight reduction of spleen weights of *Asf1b*$^{-/-}$ recipients compared with WT was observed (supplemental Figure 4H). Furthermore, the reduced leukemia burden was observed in *Asf1b*$^{-/-}$ recipients with and without IL-1β treatment (supplemental Figure 4I). Overall, these data suggest that ASF1B is one of the mediators of IL-1β–driven AML progression, and the suppression of ASF1B delayed leukemia progression at a steady state and under inflammatory stress whereas healthy hematopoiesis was not affected.

Genetic targeting of TLK1 and TLK2 suppresses AML growth and leukemic burden

ASF1A and ASF1B are known substrates of the TLKs, which have been proposed to be promising targets for various cancer types.[13,14,19] To examine whether TLK1 and TLK2 are also required for AML cell growth and survival, we used doxycycline-inducible shRNA hairpins to knock down *TLK1*, *TLK2*, or both, in MOLM-14 cells. As expected, we observed reduced phosphorylation of ASF1A upon knockdown of either *TLK1*, *TLK2*, or both. There was no significant change in total ASF1A and ASF1B protein levels (Figure 4A-B). We observed an increased intensity of the lower band for ASF1A upon *TLK1* and *TLK2*, or double knockdown, which might be because the knockdown of both TLKs may reduce levels of phosphorylated ASF1A and the lower band represents a nonphosphorylated form. Similar to ASF1 knockdown and consistent with their role in regulating ASF1 function, depletion of *TLK1*, *TLK2*, or both, resulted in a

Figure 2 (continued) by plating MOLM-14 cells expressing shASF1A, shASF1B, or both in the methylcellulose-based medium following doxycycline-induced knockdown for 14 days. (G) MOLM-14 cells expressing shASF1A, shASF1B, or both were xenografted into sublethally irradiated NSG mice, which were randomly divided into 2 groups (n = 4-5 per group) with or without 625 mg/kg doxycycline chow. All the mice were euthanized 18 days after treatment. (H-I) The leukemic burden was determined by GFP and/or RFP positivity, human CD13/CD33, and CD15 positivity using flow cytometry. (J) Spleen weight and representative images of the spleens are shown from each group. Data are expressed as means ± SEM and the Student *t* tests were used for statistical analyses. $^{**}P < .01$ and $^{***}P < .001$.

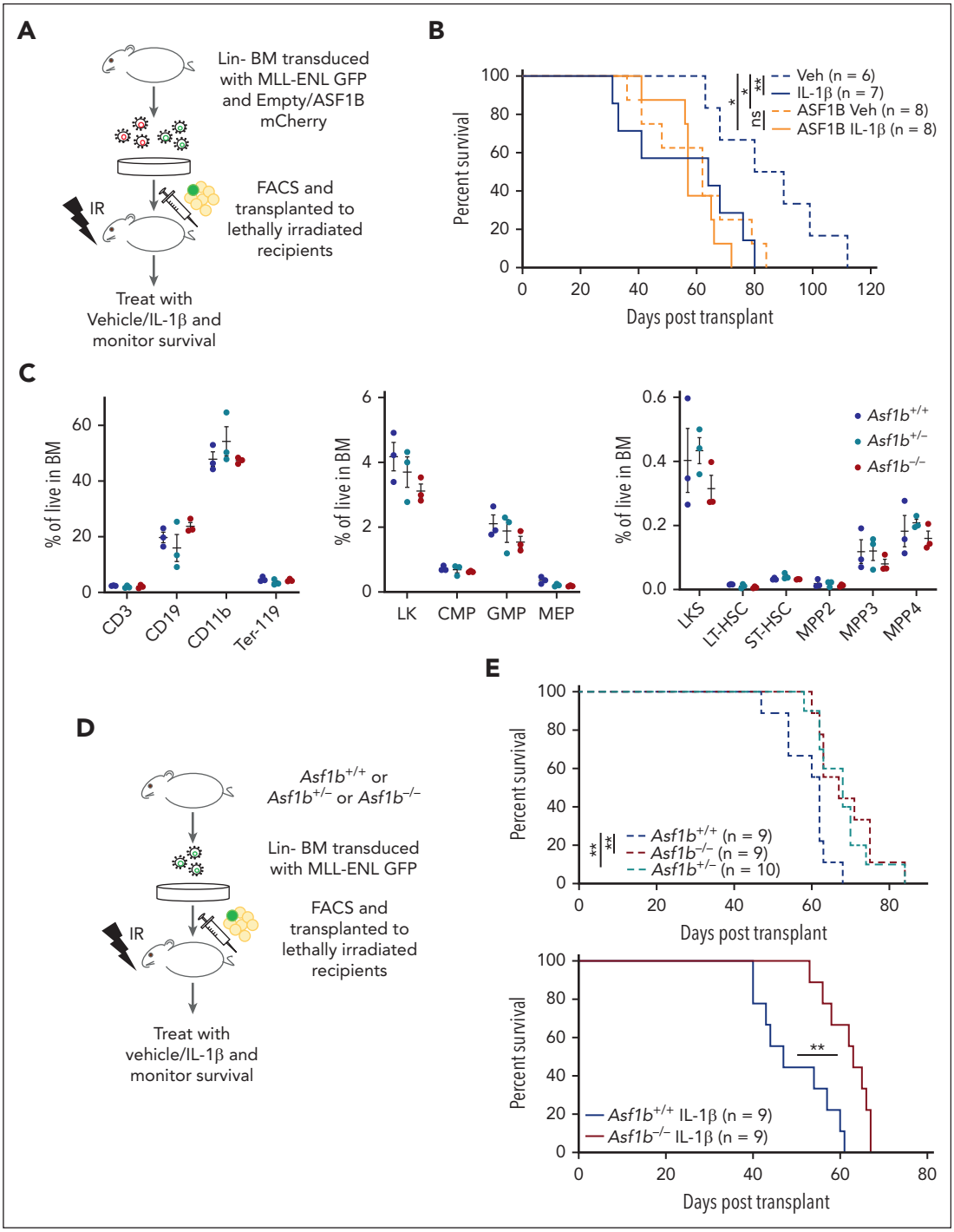

Figure 3. ASF1B potentiated IL-1–driven AML progression in a murine model of leukemia, and the absence of ASF1B attenuated the leukemia progression. (A) A schematic representation of a murine AML bone marrow transduction/transplantation model mimicking ASF1B overexpression. Lineage (Lin^-)-depleted wild-type bone marrow cells were transduced with MSCV-IRES-mCherry or MSCV-IRES-ASF1B-mCherry and MSCV-IRES-MLL-ENL-GFP constructs. After 48 hours of transduction, 10 000 sorted $mCherry^+GFP^+$ cells and supporting cells were injected into lethally irradiated C57BL/6 recipients. After engraftment confirmation, recipient mice were treated with 0.25 μg IL-1β or vehicle and monitored daily. The recipient mice were euthanized when they appeared moribund or showed signs of sickness. (B) Kaplan-Meier survival curve of recipient mice. The log-rank test was used for statistical analysis. *$P < .05$ and **$P < .01$ (C) Immunophenotyping of *Asf1b*$^{+/+}$, *Asf1b*$^{+/-}$, and *Asf1b*$^{-/-}$ mice representing different cell populations in the bone marrow. The distribution of stem and progenitor cells in the bone marrow of *Asf1b*$^{+/+}$, *Asf1b*$^{+/-}$, and *Asf1b*$^{-/-}$ mice was measured by flow cytometry. (D) A schematic representation of a murine AML bone marrow transduction/transplantation model to study the effect of ASF1B deletion on leukemia progression. Lineage (Lin^-)-depleted *Asf1b*$^{+/+}$, *Asf1b*$^{+/-}$, and *Asf1b*$^{-/-}$ bone marrow cells were transduced with MSCV-IRES-MLL-ENL-GFP retrovirus. After 48 hours of transduction, 25 000 sorted Lin^-GFP^+ cells and supporting cells were injected into lethally irradiated C57BL/6 recipients. After engraftment confirmation, recipient mice were treated with 0.25 μg IL-1β or vehicle and monitored daily. (E) Kaplan-Meier survival curve of recipient mice. The log-rank test was used for statistical analysis. **$P < .01$.

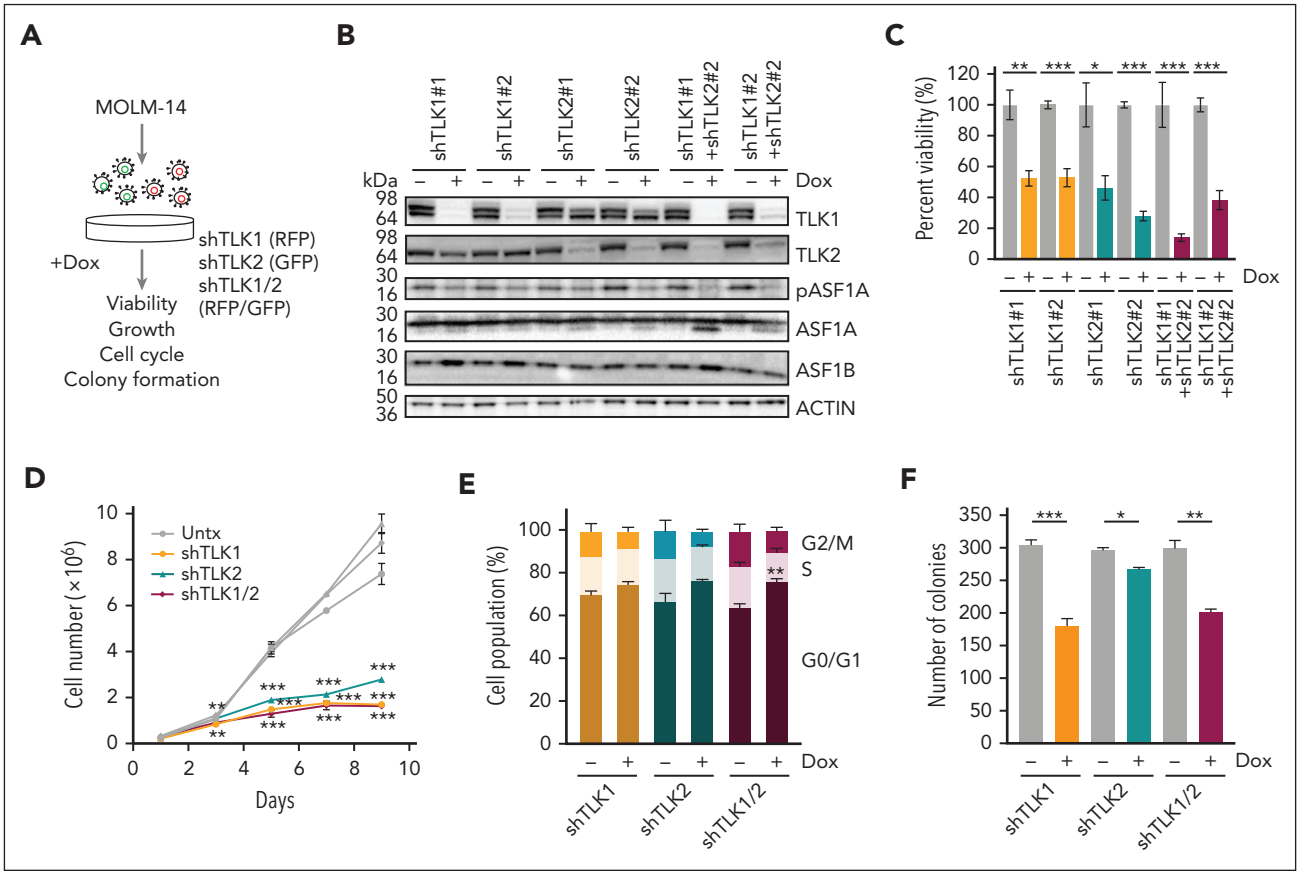

Figure 4. Reduced expression of TLKs suppresses in vitro and in vivo AML growth and leukemia burden using human cells. (A) A schematic representation of a doxycycline-inducible shRNA model targeting *TLK1*, *TLK2*, or both *TLK1* and *TLK2* in MOLM-14 cells. (B) MOLM-14 cells were treated with 1 μg/mL doxycycline for 6 days to induce knockdown. The effect of the knockdown was measured by immunoblotting analysis. (C) Cell viability of MOLM-14 cells expressing shTLK1, shTLK2, or both was measured by colorimetric (MTS) assay after 6 days of doxycycline-induced knockdown. (D) Cell growth over time of MOLM-14 cells expressing shTLK1, shTLK2, or both was indicated by cell counts. (E) Cell cycle analysis of MOLM-14 cells expressing shTLK1, shTLK2, or both using propidium iodide and flow cytometry after 6 days of doxycycline-induced knockdown. (F) Colony formation was assessed by plating cells in methylcellulose-based medium after doxycycline-induced knockdown for 14 days. Data are expressed as means ± SEM. **P* < .05, ***P* < .01, and ****P* < .001.

significant reduction of AML cell viability, cell expansion, colony formation ability, and cell cycle progression at the G0/G1 stage (Figure 4C-F). In addition to MOLM-14 cells, we observed reduced viability for *TLK2*-depleted and *TLK1/2*-depleted MONOMAC-1 cells and a trend for *TLK1*-depleted MONOMAC-1 cells. (supplemental Figure 5A). Viability was also reduced in a sample from patient with *TLK2*-depleted AML (supplemental Figure 5B). Although overexpression of ASF1A was able to rescue the effect of ASF1A knockdown on the viability of MOLM14 cells, a nonphosphorylated form of ASF1A was unable to do so. Interestingly, both wild-type ASF1A and nonphosphorylated form of ASF1A were unable to rescue the effect of TLK2 knockdown on cell viability. These results suggest that ASF1A does not rescue the phenotypes of TLK2 knockdown and 1 possibility is that TLK2 also phosphorylates other substrates. Additionally, TLK1 may also retain its function in TLK2 knockdown cells (supplemental Figure 5C-E).

TLK2 is a mediator of IL-1β–driven AML progression

We show that primary AML samples have higher protein levels of TLK1 and TLK2, with greater change in TLK2 than TLK1 levels in AML compared with in healthy cells (Figure 1E). Additionally, the combined knockdown of TLK1 and TLK2 did not confer much stronger growth defects than the TLK2 knockdown alone (Figure 4C-D). CRISPR database analysis showed higher dependency on *TLK2* than *TLK1* in AML cells (supplemental Figure 1B). Therefore, we asked whether TLK2 loss would impair AML progression. Because complete deletion of *Tlk2* is embryonically lethal, we crossed $Tlk2^{fl/fl}$ mice with *Vav-Cre* mice[35] to conditionally delete *Tlk2* in hematopoietic cells. *Vav-Cre* $Tlk2^{fl/+}$ referred to as $Tlk2^{+/-}$, and *Vav-Cre* $Tlk2^{fl/fl}$ referred to as $Tlk2^{-/-}$. Immunophenotyping of $Tlk2^{-/-}$ mice showed slightly lower B-cell numbers than controls but were comparable in other cell types, including stem and progenitor cells (supplemental Figure 6A-C). We did not observe growth differences between CRISPR-edited *Tlk2* cells compared with nontargeting cells in competition assays in vitro (supplemental Figure 6D). Using the MLL-ENL murine model of AML (Figure 5A), heterozygous and homozygous deletion of *Tlk2* (median survival, 138 days and 187 days, respectively) significantly extended the survival compared with wild-type recipients (median survival, 84 days; $P = .006$ and $P < .0001$, respectively). These data suggest that *Tlk2* is haploinsufficient for AML progression and even a 50% reduction in expression or activity might improve the survival of the patients. IL-1β treatment promoted AML progression in both wild-type and $Tlk2^{-/-}$ mice

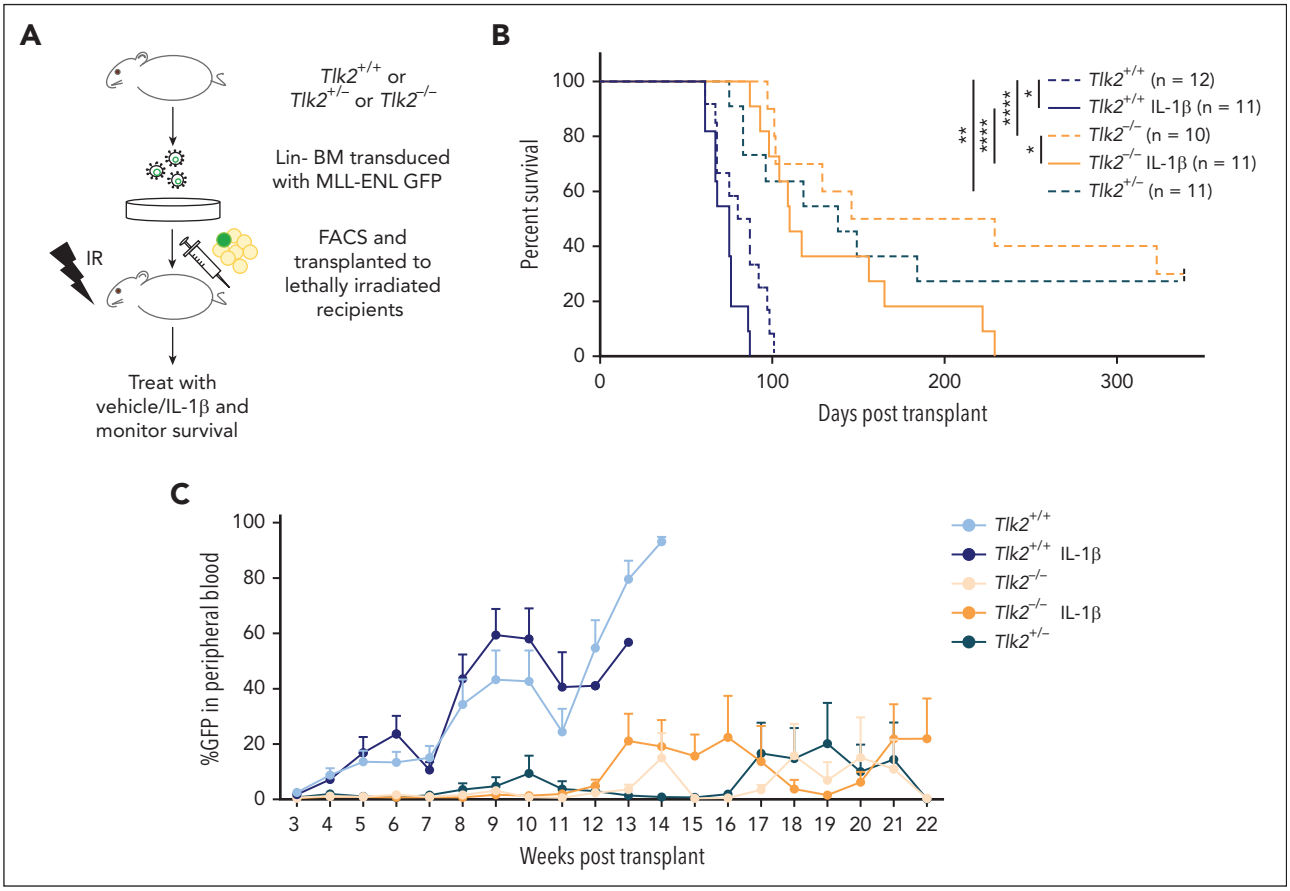

Figure 5. The absence of TLK2 attenuates leukemia burden and IL-1β–driven AML progression in a murine model of leukemia. (A) A schematic representation of a murine AML bone marrow transduction/transplantation model to study the effect of TLK2 deletion on leukemia progression. Lineage-depleted *Tlk2*$^{+/+}$, *Tlk2*$^{+/-}$, *Tlk2*$^{-/-}$ bone marrow cells were transduced with MSCV-IRES-MLL-ENL-GFP retrovirus. After 48 hours of transduction, 15 000 sorted Lin$^-$GFP$^+$ cells and supporting cells were injected into lethally irradiated C57BL/6 recipients. After engraftment confirmation, recipient mice were treated with 0.25 μg IL-1β or vehicle and monitored daily. (B) Kaplan-Meier survival curve of recipient mice. The log-rank test was used for statistical analysis. (C) The percentage of leukemic cells in the peripheral blood over time was measured by flow cytometry. *P < .05, **P < .01, and ****P < .0001.

compared with vehicle-treated mice (median survival for wild-type, 75 days vs 83 days, P = .033; and median survival for *Tlk2*$^{-/-}$, 110 days vs 187 days, P = .046). However, *Tlk2* deficiency significantly extended the survival of IL-1β–treated mice compared with IL-1β–treated wild-type mice (median survival, 110 vs 75 days; P < .0001; Figure 5B). Weekly analysis of leukemic burden in the peripheral blood confirmed that heterozygous and homozygous deletion of *Tlk2* led to slower leukemia progression compared with wild-type mice (Figure 5C). At the end point, spleen weight and leukemic burden measured by GFP$^+$ cells were comparable between each group (supplemental Figure 6E-F). Furthermore, the flow cytometry analysis of bone marrow cells at the end point showed that *Tlk2*$^{-/-}$ mice bone marrow cells have reduced lineage-negative cells but that these cells go through apoptosis at a similar rate as *Tlk2*$^{+/+}$ cells. The reduced lineage-negative cells might be responsible for the reduced leukemia burden for the mice (supplemental Figure 6G-H). To further understand how TLK2 deletion in the MLL-ENL model affects serial transplantability, we performed a secondary transplantation study. We observed prolonged survival of *Tlk2*$^{-/-}$ mice (supplemental Figure 6I). However, in contrast to the primary transplant, *Tlk2*$^{+/-}$ did not extend survival compared with *Tlk2*$^{+/+}$ mice, suggesting that efficient targeting of TLK2 is needed to gain effective and long-term effects as a therapeutic target. Taken together, our results showed depletion of TLK2 significantly delayed IL-1β–driven AML progression.

Depletion of ASF1A/B or TLK1/2 leads to changes in the protein and phosphoprotein signaling related to the cell cycle and DNA damage response in AML

To assess how ASF1s or TLKs deficiency reduced cell growth in vitro and prolonged survival in vivo in AML, we performed global proteomics and phosphoproteomics analyses after the depletion of ASF1s or TLKs in MOLM-14 cells. Upon ASF1A, ASF1B, or ASF1A/B knockdown (supplemental Figure 7A), we observed changes in the levels of 1455, 3335, and 3304 proteins, and 5553, 3699, and 2444 phosphorylation sites, respectively, compared with nontargeting controls (supplemental Table 6). KEGG pathway analysis of altered proteins identified enrichments in the categories of down-regulation of the cell cycle, DNA replication, and DNA repair pathways (supplemental Figure 7B). We narrowed our STRING-DB Gene Ontology analysis to ASF1A/B knockdown, which revealed that ASF1A/B knockdown led to decreased protein levels and phosphorylation of proteins associated with the cell

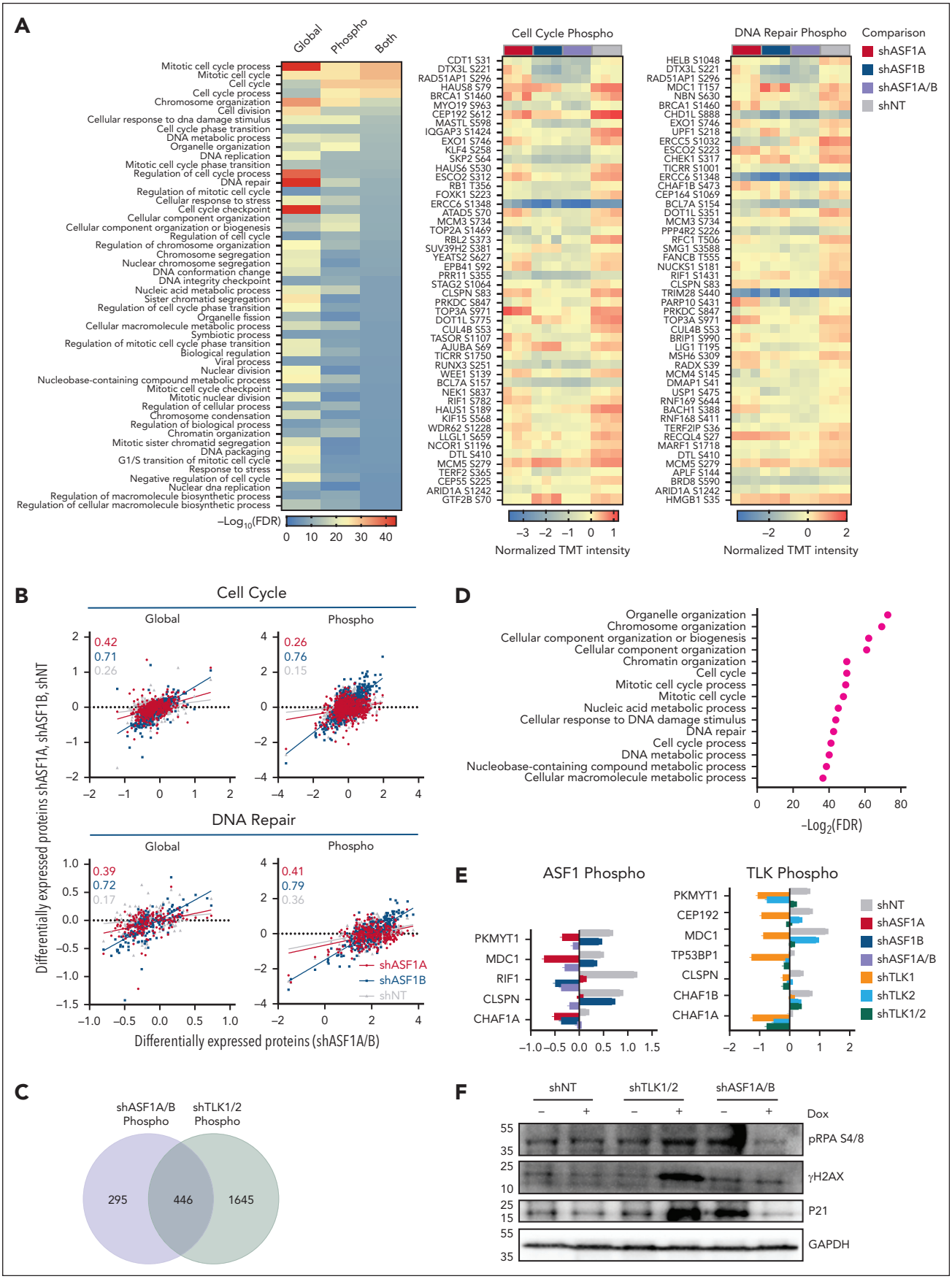
A
Global
Phospho
Both
Mitotic cell cycle process
Mitotic cell cycle
Cell cycle
Cell cycle process
Chromosome organization
Cell division
Cellular response to dna damage stimulus
Cell cycle phase transition
DNA metabolic process
Organelle organization
DNA replication
Mitotic cell cycle phase transition
Regulation of cell cycle process
DNA repair
Regulation of mitotic cell cycle
Cellular response to stress
Cell cycle checkpoint
Cellular component organization
Cellular component organization or biogenesis
Regulation of cell cycle
Regulation of chromosome organization
Chromosome segregation
Nuclear chromosome segregation
DNA conformation change
DNA integrity checkpoint
Nucleic acid metabolic process
Sister chromatid segregation
Regulation of cell cycle phase transition
Organelle fission
Cellular macromolecule metabolic process
Symbiotic process
Regulation of mitotic cell cycle phase transition
Biological regulation
Viral process
Nuclear division
Nucleobase-containing compound metabolic process
Mitotic cell cycle checkpoint
Mitotic nuclear division
Regulation of cellular process
Chromosome condensation
Regulation of biological process
Chromatin organization
Mitotic sister chromatid segregation
DNA packaging
G1/S transition of mitotic cell cycle
Response to stress
Negative regulation of cell cycle
Nuclear dna replication
Regulation of macromolecule biosynthetic process
Regulation of cellular macromolecule biosynthetic process
−Log10(FDR)
0 10 20 30 40
Cell Cycle Phospho
CDT1 S31
DTX3L S221
RAD51AP1 S296
HAUS8 S79
BRCA1 S1460
MYO19 S963
CEP192 S612
MASTL S598
IQGAP3 S1424
EXO1 S746
KLF4 S258
SKP2 S64
HAUS6 S530
ESCO2 S312
RB1 T356
FOXK1 S223
ERCC6 S1348
ATAD5 S70
MCM3 S734
TOP2A S1469
RBL2 S373
SUV39H2 S381
YEATS2 S627
EPB41 S92
PRR11 S355
STAG2 S1064
CLSPN S83
PRKDC S847
TOP3A S971
DOT1L S775
CUL4B S53
TASOR S1107
AJUBA S69
TICRR S1750
RUNX3 S251
WEE1 S139
BCL7A S157
NEK1 S837
RIF1 S782
HAUS1 S189
KIF15 S568
WDR62 S1228
LLGL1 S659
NCOR1 S1196
DTL S410
MCM5 S279
TERF2 S365
CEP55 S225
ARID1A S1242
GTF2B S70
−3 −2 −1 0 1
Normalized TMT intensity
DNA Repair Phospho
HELB S1048
DTX3L S221
RAD51AP1 S296
MDC1 T157
NBN S630
BRCA1 S1460
CHD1L S888
EXO1 S746
UPF1 S218
ERCC5 S1032
ESCO2 S223
CHEK1 S317
TICRR S1001
ERCC6 S1348
CHAF1B S473
CEP164 S1069
BCL7A S154
DOT1L S351
MCM3 S734
PPP4R2 S226
RFC1 T506
SMG1 S3588
FANCB T555
NUCKS1 S181
RIF1 S1431
CLSPN S83
TRIM28 S440
PARP10 S431
PRKDC S847
TOP3A S971
CUL4B S53
BRIP1 S990
LIG1 T195
MSH6 S309
RADX S39
MCM4 S145
DMAP1 S41
USP1 S475
RNF169 S644
BACH1 S388
RNF168 S411
TERF2IP S36
RECQL4 S27
MARF1 S1718
DTL S410
MCM5 S279
APLF S144
BRD8 S590
ARID1A S1242
HMGB1 S35
−2 0 2
Normalized TMT intensity
Comparison
shASF1A
shASF1B
shASF1A/B
shNT
B
Cell Cycle
Global
Phospho
0.42
0.71
0.26
0.26
0.76
0.15
DNA Repair
Global
Phospho
0.39
0.72
0.17
0.41
0.79
0.36
shASF1A
shASF1B
shNT
Differentially expressed proteins shASF1A, shASF1B, shNT
Differentially expressed proteins (shASF1A/B)
D
Organelle organization
Chromosome organization
Cellular component organization or biogenesis
Cellular component organization
Chromatin organization
Cell cycle
Mitotic cell cycle process
Mitotic cell cycle
Nucleic acid metabolic process
Cellular response to DNA damage stimulus
DNA repair
Cell cycle process
DNA metabolic process
Nucleobase-containing compound metabolic process
Cellular macromolecule metabolic process
0 20 40 60 80
−Log2(FDR)
E
ASF1 Phospho
PKMYT1
MDC1
RIF1
CLSPN
CHAF1A
−1.0 −0.5 0.0 0.5 1.0 1.5
TLK Phospho
PKMYT1
CEP192
MDC1
TP53BP1
CLSPN
CHAF1B
CHAF1A
−2 −1 0 1 2
shNT
shASF1A
shASF1B
shASF1A/B
shTLK1
shTLK2
shTLK1/2
C
shASF1A/B Phospho
shTLK1/2 Phospho
295
446
1645
F
shNT
shTLK1/2
shASF1A/B
− + − + − +
Dox
55
35
pRPA S4/8
25
10
γH2AX
25
15
P21
55
35
GAPDH

Figure 6.

cycle (PKMYT1, CEP192) and DNA repair (RIF1, BRIP1, CHAF1B, CLSPN, MDC1) pathways, along with reductions in phosphorylation of DNA repair mediators (TP53BP1, ERCC5) (Figure 6A; supplemental Figure 7B; supplemental Tables 7 and 8). Many of these factors (RIF1, BRIP1, CHAF1B, CLSPN, and MDC1) are consistent with our finding of reduced growth and increased cell cycle arrest in G0/G1 phase upon ASF1A/B knockdown (Figure 2).[36-38] Further, several of these factors are known to be associated with ASF1A-mediated changes (MDC1 and RIF1).[39,40] However, a more significant correlation was observed between ASF1B and ASF1A/B-related changes than between ASF1A and ASF1A/B (Figure 6B). Upon TLK1, TLK2, or TLK1/2 knockdown in MOLM-14 cells, we observed 1915, 1162, and 3352 differentially expressed proteins, respectively, and 3351, 215, and 8761 changes of phosphorylation sites, respectively (supplemental Table 9). Similarly, the depletion of TLKs resulted in the downregulation of the cell cycle and DNA replication and repair pathways (supplemental Figure 7C). Furthermore, known TLK1 or TLK2 substrates ASF1A-S166, ASF1A-S175, ASF1B-S198, and RAD9-S326 were reduced in *TLK1/2*-depleted MOLM-14 cells (supplemental Figure 7D).[14,41,42] Interestingly, proteins with loss of phosphorylation in TLK1/2 had significant overlap with those with loss in ASF1A/B, 446 of 2091 proteins (Figure 6C). STRING-DB Gene Ontology analysis showed that 446 proteins with decreased phosphorylation levels in both ASF1A/B and TLK1/2 knockdown were enriched in pathways related to cell cycle regulation and DNA repair (Figure 6D; supplemental Figure 8). Specifically, we noted downregulation in the phosphoproteome pathways associated with the cell cycle and DNA repair. We observed phosphorylation of PKMYT1, CEP192, MDC1, TP53BP1, CLSPN, CHAF1B, and CHAF1A were downregulated in *TLK1/2*-depleted cells with overlapping factors (PKMYT1, MDC1, CLSPN, and CHAF1A) identified in ASF1A/B (Figure 6A,E; supplemental Figure 7E; supplemental Tables 10 and 11). Our immunoblotting data showed that the expression of DNA damage marker γH2AX and cell cycle marker p21 were elevated in *TLK1/2*-depleted MOLM-14 cells (Figure 6F). Taken cumulatively, the TLK-ASF1 signaling dysregulated the key cell cycle and DNA repair pathways upon *ASF1A/B* and *TLK1/2* depletion, which provides the mechanistic basis for the reduction in cell growth and increased survival of knockout mice in vivo.

Discussion

Despite recent improvements in targeted therapies, the 5-year survival rate for patients with AML has remained low (~29%) for the past 4 decades.[43] This is primarily because of the rapid emergence of drug-resistant mutations in leukemic cells.[2] Additionally, the bone marrow microenvironment exerts inflammatory stress and becomes growth permissive to malignant cells over healthy cells. This demands an improved understanding of disease biology and the identification of novel therapeutic targets that are effective across different AML genetic subtypes.

Previously, alterations in the TLK-ASF1 pathway were proposed to contribute to cancer initiation, development, and progression in a variety of cancer types, including breast, colorectal, prostate, melanoma, and cervical squamous cell carcinoma.[18,19,44-46] However, the role of the TLK-ASF1 pathway in leukemia and hematopoiesis has not been extensively investigated. In this study we show that aberrant IL-1β signaling drives AML progression by upregulating the TLK-ASF1 histone chaperone pathway. We show that knocking down of either ASF1 or TLK impaired cell growth and survival in both in vitro and in vivo models of AML, representing multiple genetic subtypes of AML. Furthermore, depletion of ASF1B or TLK2 impaired IL-1β–driven AML progression in a murine model, highlighting the potential of targeting the TLK-ASF1 pathway as a novel therapeutic target for AML.

Interestingly, our results indicate that heterozygous or complete deletion of either ASF1B or its regulator, TLK2, delays AML progression at a steady state and under inflammatory stress using IL-1β, suggesting an enhanced dependency of AML on the TLK-ASF1 pathway. Previous work showed that overexpression of *CHAF1B*, a subunit of the CAF-1 histone chaperone complex that interacts with ASF1B, promoted leukemia progression in a transgenic murine model of MLL-AF9–positive AML.[47] Because CAF1 is predominantly involved in replication-dependent histone deposition, these results are consistent with an enhanced dependency of AML on the TLK-ASF1 pathway. However, complete elimination of disease was not achieved upon ASF1B deletion, indicating that other factors, including ASF1A or CAF1, may contribute to AML progression in the absence of ASF1B. This is consistent with our result that ASF1A depletion has a significant impact on AML growth in vitro, and with previous observations that ASF1A depletion caused growth arrest in hepatocellular carcinoma and prostate cancer cells.[48] Additionally, we observed 2 bands in some of the ASF1A immunoblots. We suggest that the upper band may be the phosphorylated form of ASF1A because it was abolished by phosphatase treatment according to published studies.[39,49] It is possible that ASF1B knockdown may affect ASF1A phosphorylation, or it might be a dominant negative form of ASF1A. However, additional experiments are required to confirm this.

Our proteomics and phosphoproteomics analyses revealed that the TLK-ASF1 pathway promoted leukemogenesis through the

Figure 6. Global proteome and phosphoproteome alterations in AML cells upon ASF1 and TLK depletion. Global proteomics and phosphoproteomics analysis of AML cell line MOLM-14 was performed upon knockdown of ASF1s or TLKs as described in supplemental Figure 6A and "Methods." (A) STRING-DB Gene Ontology analysis for the biological process for proteins that were significantly downregulated for protein levels or their phosphorylation upon ASF1A/B knockdown (left) compared with nontargeting controls (shNT). Analysis of variance (ANOVA) *t* test, false discovery rate (FDR) <0.05. Additionally, the top 50 downregulated phosphorylation sites for the proteins associated with cell cycle (middle, GO:0007049) and DNA repair (right, GO:0006281) Gene Ontology terms are shown. Scale bar represents normalized TMT intensity using medium centering approach. If multiple phosphorylation sites of the same protein were observed, only the most downregulated phosphorylation sites were shown in the heat maps. (B) The x-axis corresponds to the normalized TMT intensity with medium centering approach of global or phosphorylated protein of all proteins that were significantly altered in shASF1A/B cells (ANOVA *t* test, FDR < 0.05), whereas the y-axis shows their normalized TMT intensity in shASF1A, shASF1B, or shNT cells. The correlation coefficients (r) are shown for shASF1A/B cells with shASF1A (red), shASF1B (blue), and shNT (gray) cells within cell cycle and DNA repair Gene Ontology terms. (C) Venn diagram showing the overlap of proteins with reduced phosphorylation in MOLM-14 cells with ASF1A/B or TLK1/2 knockdown. (D) STRING-DB Gene Ontology analysis for the biological process for the 446 proteins with reduced phosphorylation in MOLM-14 cells with both ASF1A/B or TLK1/2 knockdown. (E) Representative phosphorylated DNA damage proteins upon ASF1 and TLK knockdown. (F) Immunoblot of DNA damage and cell cycle–related proteins upon ASF1 and TLK knockdown. TMT, tandem mass tags.

regulation of the cell cycle and DNA damage responses, further supporting the TLK-ASF1 pathway's role in promoting AML progression. Moreover, we observed that TLK knockdown had a more significant impact on downstream signaling, as indicated by the modulation of a higher number of phosphorylation sites compared with ASF1 knockdown. Our results also revealed potential new substrates and interacting proteins of TLKs that might be involved in the AML progression.[48]

To our knowledge, our study is the first to investigate the role of the TLK-ASF1 pathway in inflammation-mediated AML progression. Mechanistically, we found that ASF1B expression is regulated by IL-1β in a p38MAPK-dependent manner, and that transcription factors MYBL2 and E2F1 may be responsible for the transcriptional upregulation of *ASF1B*.

Importantly, we demonstrated that targeting the TLK-ASF1 pathway effectively reduces leukemia burden and progression in vivo, presenting a promising therapeutic target for AML. Previous work identified the feasibility of targeting ASF1 using a peptide inhibitor that binds to the histone binding pocket and reduces tumor size in vivo.[50] Several nonspecific small-molecule inhibitors targeting TLK1 and TLK2 have been tested in the breast cancer models[19,51] and recent studies have reported more potent versions of TLK inhibitors,[52,53] although their specificity and overall suitability for in vivo use remain unclear.

In summary, our study reveals that chronic inflammation alters the transcriptional landscape of AML and healthy progenitors, thereby driving disease progression. We identified the TLK-ASF1 pathway as a critical mediator in IL-1β–driven leukemia progression and demonstrated that the modulation of this pathway is a novel strategy to prevent inflammatory stress–mediated AML progression without affecting healthy cells. These findings contribute to our understanding of AML biology and provide a foundation for the development of targeted therapies against AML by specifically targeting the TLK-ASF1 pathway.

Acknowledgments

The authors thank all the patients for donating precious samples. RNA quality assessments, library creation, and short-read sequencing assays were performed by the OHSU Massively Parallel Sequencing Shared Resource. The authors also thank the OHSU flow cytometer core, transgenic core, and the OHSU Department of Comparative Medicine and vivarium staff for taking care of the animal colonies. The authors thank Anja Groth for supplying the anti-pS166 ASF1A antibody, and Jeffrey Tyner for sharing AML samples.

Funding for this project was provided by the National Institutes of Health (NIH), National Cancer Institute (NCI) (grant R01 CA229875-01A1); the American Cancer Society (RSG-17-187-01-LIB); V Foundation Scholar award; and the Knight Cancer Research Institute, Oregon Health & Science University as pilot research projects; the Exploratory seed grant award; and Tartar Trust Foundation. A. Agarwal is supported by grants from the NIH, National Heart, Lung, and Blood Institute (NHLBI) (R01 HL155426), Alex's Lemonade Stand/RUNX1 Research Foundation, Edward P. Evans Foundation, Chan Zuckerberg Initiative Funds, as well as NIH, NCI consortia grants U54 CA224019 (S.M., A. Agarwal) and U01 CA257666, and the NIH, NCI's Office of Cancer Clinical Proteomics Research (Clinical Proteomic Tumor Analysis Consortium) under NIH, NCI grants U01CA214116 and U01CA271412 (S.G., A. Agarwal). H.-Y.L. was supported by a Cancer Biology Stipend from OHSU. M.M. and J.M. are supported by NIH, NHLBI NRSAF31 grants 1F31HL162542 and 1F31HL164052, respectively. M.M. was funded through NIH, NCI T32 grant T32CA254888. T.H.S. was funded by the Spanish Ministry of Science, Innovation and Universities (PGC2018-095616-B-I00/GINDATA and FEDER), received institutional support from the Centres of Excellence Severo Ochoa award, and the CERCA Programme and funding from the Intramural Research Program of the NIH, NCI (ZIA BC 012010). M.V.-P. was funded by an FPI fellowship from the Ministry of Science, Innovation and Universities and support from the IRB Barcelona.

Authorship

Contribution: A. Agarwal provided project oversight for experimental design, data management, data analysis and interpretation, and methods development; A. Agarwal, H.-Y.L., M.M., J.M., M.V.-P., S.J., D.B., C.-F.T., C.P., J.J., A. Adey, S.G., T.L., S.M., and T.H.S. helped with workflow development, experiments, data processing, management, and analysis; and all authors wrote the manuscript and provided feedback.

Conflict-of-interest disclosure: The authors declare no competing financial interests.

ORCID profiles: H.-Y.L., 0000-0002-6322-1826; M.V.-P., 0000-0002-7288-4197; S.G., 0000-0002-6534-4774; S.M., 0000-0001-8333-6607; A. Agarwal, 0000-0002-8319-6162.

Correspondence: Anupriya Agarwal, Knight Cancer Institute, Oregon Health & Science University, 3181 SW Sam Jackson Park Rd, KR-HEM, Portland, OR 97239; email: agarwala@ohsu.edu.

Footnotes

The accession number for RNA-seq data sets reported in this paper is: phs001657.v2.p1.

All analysis was done using R and the leapR package, which can be found here: https://github.com/PNNL-CompBio/leapR. Further infor-mation can be obtained from, and requests for resources and reagents should be directed to and will be fulfilled by, the corresponding author, Anupriya Agarwal (agarwala@ohsu.edu).

REFERENCES

1. Estey E, Dohner H. Acute myeloid leukaemia. *Lancet*. 2006;368(9550):1894-1907.

2. McMahon CM, Ferng T, Canaani J, et al. Clonal selection with RAS pathway activation mediates secondary clinical resistance to selective FLT3 inhibition in acute myeloid leukemia. *Cancer Discov*. 2019;9(8):1050-1063.

3. Carter BZ, Mak PY, Wang X, et al. An ARC-regulated IL1beta/Cox-2/PGE2/beta-catenin/ARC circuit controls leukemia-microenvironment interactions and confers drug resistance in AML. *Cancer Res*. 2019;79(6):1165-1177.

4. Kristinsson SY, Bjorkholm M, Hultcrantz M, Derolf AR, Landgren O, Goldin LR. Chronic immune stimulation might act as a trigger for the development of acute myeloid leukemia or myelodysplastic syndromes. *J Clin Oncol*. 2011;29(21):2897-2903.

5. Trowbridge JJ, Starczynowski DT. Innate immune pathways and inflammation in

hematopoietic aging, clonal hematopoiesis, and MDS. *J Exp Med*. 2021;218(7): e20201544.

6. Caiado F, Pietras EM, Manz MG. Inflammation as a regulator of hematopoietic stem cell function in disease, aging, and clonal selection. *J Exp Med*. 2021;218(7): e20201541.
7. Carey A, Edwards DKt, Eide CA, et al. Identification of interleukin-1 by functional screening as a key mediator of cellular expansion and disease progression in acute myeloid leukemia. *Cell Rep*. 2017;18(13): 3204-3218.
8. Barreyro L, Will B, Bartholdy B, et al. Overexpression of IL-1 receptor accessory protein in stem and progenitor cells and outcome correlation in AML and MDS. *Blood*. 2012;120(6):1290-1298.
9. Hosseini MM, Kurtz SE, Abdelhamed S, et al. Inhibition of interleukin-1 receptor-associated kinase-1 is a therapeutic strategy for acute myeloid leukemia subtypes. *Leukemia*. 2018; 32(11):2374-2387.
10. Fang J, Bolanos LC, Choi K, et al. Ubiquitination of hnRNPA1 by TRAF6 links chronic innate immune signaling with myelodysplasia. *Nat Immunol*. 2017;18(2): 236-245.
11. Groth A, Corpet A, Cook AJ, et al. Regulation of replication fork progression through histone supply and demand. *Science*. 2007; 318(5858):1928-1931.
12. Park YJ, Luger K. Histone chaperones in nucleosome eviction and histone exchange. *Curr Opin Struct Biol*. 2008;18(3):282-289.
13. Segura-Bayona S, Stracker TH. The Tousled-like kinases regulate genome and epigenome stability: implications in development and disease. *Cell Mol Life Sci*. 2019;76(19): 3827-3841.
14. Klimovskaia IM, Young C, Strømme CB, et al. Tousled-like kinases phosphorylate Asf1 to promote histone supply during DNA replication. *Nat Commun*. 2014;5:3394.
15. English CM, Adkins MW, Carson JJ, Churchill ME, Tyler JK. Structural basis for the histone chaperone activity of Asf1. *Cell*. 2006; 127(3):495-508.
16. Pilyugin M, Demmers J, Verrijzer CP, Karch F, Moshkin YM. Phosphorylation-mediated control of histone chaperone ASF1 levels by Tousled-like kinases. *PLoS One*. 2009;4(12): e8328.
17. Simon B, Lou HJ, Huet-Calderwood C, et al. Tousled-like kinase 2 targets ASF1 histone chaperones through client mimicry. *Nat Commun*. 2022;13(1):749.
18. Corpet A, De Koning L, Toedling J, et al. Asf1b, the necessary Asf1 isoform for proliferation, is predictive of outcome in breast cancer. *EMBO J*. 2011;30(3):480-493.
19. Kim JA, Tan Y, Wang X, et al. Comprehensive functional analysis of the tousled-like kinase 2 frequently amplified in aggressive luminal breast cancers. *Nat Commun*. 2016;7:12991.
20. Lee SB, Segura-Bayona S, Villamor-Paya M, et al. Tousled-like kinases stabilize replication forks and show synthetic lethality with checkpoint and PARP inhibitors. *Sci Adv*. 2018;4(8):eaat4985.
21. Segura-Bayona S, Knobel PA, Gonzalez-Buron H, et al. Differential requirements for Tousled-like kinases 1 and 2 in mammalian development. *Cell Death Differ*. 2017;24(11): 1872-1885.
22. Agarwal A, Bumm TG, Corbin AS, et al. Absence of SKP2 expression attenuates BCR-ABL-induced myeloproliferative disease. *Blood*. 2008;112(5):1960-1970.
23. Agarwal A, Fleischman AG, Petersen CL, et al. Effects of plerixafor in combination with BCR-ABL kinase inhibition in a murine model of CML. *Blood*. 2012;120(13):2658-2668.
24. Agarwal A, Mackenzie RJ, Besson A, et al. BCR-ABL1 promotes leukemia by converting p27 into a cytoplasmic oncoprotein. *Blood*. 2014;124(22):3260-3273.
25. Szklarczyk D, Gable AL, Nastou KC, et al. The STRING database in 2021: customizable protein-protein networks, and functional characterization of user-uploaded gene/ measurement sets. *Nucleic Acids Res*. 2021; 49(D1):D605-D612.
26. Liu X, Song J, Zhang Y, et al. ASF1B promotes cervical cancer progression through stabilization of CDK9. *Cell Death Dis*. 2020;11(8):705.
27. Ma J, Han W, Lu K. Comprehensive pan-cancer analysis and the regulatory mechanism of ASF1B, a gene associated with thyroid cancer prognosis in the tumor micro-environment. *Front Oncol*. 2021;11: 711756.
28. Tsherniak A, Vazquez F, Montgomery PG, et al. Defining a cancer dependency map. *Cell*. 2017;170(3):564-576.e16.
29. Tyner JW, Tognon CE, Bottomly D, et al. Functional genomic landscape of acute myeloid leukaemia. *Nature*. 2018;562(7728): 526-531.
30. Kuleshov MV, Jones MR, Rouillard AD, et al. Enrichr: a comprehensive gene set enrichment analysis web server 2016 update. *Nucleic Acids Res*. 2016;44(W1):W90-W97.
31. Hayashi R, Goto Y, Tanaka R, Oonogi K, Hisasue M, Yoshida K. Transcriptional regulation of human chromatin assembly factor ASF1. *DNA Cell Biol*. 2007;26(2):91-99.
32. Zou Z, Ohta T, Miura F, Oki S. ChIP-Atlas 2021 update: a data-mining suite for exploring epigenomic landscapes by fully integrating ChIP-seq, ATAC-seq and Bisulfite-seq data. *Nucleic Acids Res*. 2022; 50(W1):W175-W182.
33. Cancer Genome Atlas Research Network, Ley TJ, Miller C, et al. Genomic and epigenomic landscapes of adult de novo acute myeloid leukemia. *N Engl J Med*. 2013; 368(22):2059-2074.
34. Zuber J, Radtke I, Pardee TS, et al. Mouse models of human AML accurately predict chemotherapy response. *Genes Dev*. 2009; 23(7):877-889.
35. Bustelo XR, Rubin SD, Suen KL, Carrasco D, Barbacid M. Developmental expression of the vav protooncogene. *Cell Growth Differ*. 1993;4(4):297-308.
36. Rizeq B, Sif S, Nasrallah GK, Ouhtit A. Novel role of BRCA1 interacting C-terminal helicase 1 (BRIP1) in breast tumour cell invasion. *J Cell Mol Med*. 2020;24(19):11477-11488.
37. Foti R, Gnan S, Cornacchia D, et al. Nuclear architecture organized by Rif1 underpins the replication-timing program. *Mol Cell*. 2016; 61(2):260-273.
38. Ulsamer A, Martinez-Limon A, Bader S, et al. Regulation of Claspin by the p38 stress-activated protein kinase protects cells from DNA damage. *Cell Rep*. 2022;40(12):111375.
39. Lee KY, Dutta A. Chk1 promotes non-homologous end joining in G1 through direct phosphorylation of ASF1A. *Cell Rep*. 2021; 34(4):108680.
40. Tang M, Chen Z, Wang C, et al. Histone chaperone ASF1 acts with RIF1 to promote DNA end-joining in BRCA1-deficient cells. *J Biol Chem*. 2022;298(6):101979.
41. Sillje HH, Nigg EA. Identification of human Asf1 chromatin assembly factors as substrates of Tousled-like kinases. *Curr Biol*. 2001; 11(13):1068-1073.
42. Kelly R, Davey SK. Tousled-like kinase-dependent phosphorylation of Rad9 plays a role in cell cycle progression and G2/M checkpoint exit. *PLoS One*. 2013;8(12): e85859.
43. Viale PH. The American Cancer Society's facts & figures: 2020 edition. *J Adv Pract Oncol*. 2020;11(2):135-136.
44. Li F, Huang Q, Luster TA, et al. In vivo epigenetic CRISPR screen identifies Asf1a as an immunotherapeutic target in Kras-mutant lung adenocarcinoma. *Cancer Discov*. 2020; 10(2):270-287.
45. Yang S, Liu L, Cao C, et al. USP52 acts as a deubiquitinase and promotes histone chaperone ASF1A stabilization. *Nat Commun*. 2018;9(1):1285.
46. Khalil MI, De Benedetti A. Tousled-like kinase 1: a novel factor with multifaceted role in mCRPC progression and development of therapy resistance. *Cancer Drug Resist*. 2022; 5(1):93-101.
47. Volk A, Liang K, Suraneni P, et al. A CHAF1B-dependent molecular switch in hematopoiesis and leukemia pathogenesis. *Cancer Cell*. 2018;34(5):707-723.e7.
48. Wu Y, Li X, Yu J, Bjorkholm M, Xu D. ASF1a inhibition induces p53-dependent growth arrest and senescence of cancer cells. *Cell Death Dis*. 2019;10(2):76.
49. Huang TH, Fowler F, Chen CC, Shen ZJ, Sleckman B, Tyler JK. The histone chaperones ASF1 and CAF-1 promote

MMS22L-TONSL-mediated Rad51 loading onto ssDNA during homologous recombination in human cells. *Mol Cell*. 2018; 69(5):879-892.e5.

50. Bakail M, Gaubert A, Andreani J, et al. Design on a rational basis of high-affinity peptides inhibiting the histone chaperone ASF1. *Cell Chem Biol*. 2019;26(11):1573-1585.e10.

51. Mortuza GB, Hermida D, Pedersen AK, et al. Molecular basis of Tousled-like kinase 2 activation. *Nat Commun*. 2018;9(1):2535.

52. Lee SB, Chang TY, Lee NZ, Yu ZY, Liu CY, Lee HY. Design, synthesis and biological evaluation of bisindole derivatives as anticancer agents against Tousled-like kinases. *Eur J Med Chem*. 2022;227: 113904.

53. Singh V, Bhoir S, Chikhale RV, et al. Generation of phenothiazine with potent anti-TLK1 activity for prostate cancer therapy. *iScience*. 2020;23(9):101474.